Physics Letters A 374 (2010) 3538–3545

Contents lists available at ScienceDirect

Physics Letters A

www.elsevier.com/locate/pla

Conducting to non-conducting transition in dual transmission lines using a ternary model with long-range correlated disorder

E. Lazo [a,*], E. Diez [b]

[a] Departamento de Física, Facultad de Ciencias, Universidad de Tarapacá, Arica, Chile
[b] Departamento de Física Fundamental, Universidad de Salamanca, Salamanca, E-37008, Spain

ARTICLE INFO

Article history:
Received 27 April 2010
Received in revised form 6 June 2010
Accepted 14 June 2010
Available online 19 June 2010
Communicated by R. Wu

Keywords:
Localization–delocalization transition
Disordered electrical circuits
Long-range correlations

ABSTRACT

In this work we study the behavior of the allowed and forbidden frequencies in disordered classical dual transmission lines when the values of capacitances $\{C_j\}$ are distributed according to a ternary model with long-range correlated disorder. We introduce the disorder from a random sequence with a power spectrum $S(k) \propto k^{-(2\alpha-1)}$, where $\alpha \geqslant 0.5$ is the correlation exponent. From this sequence we generate an asymmetric ternary map using two map parameters b_1 and b_2, which adjust the occupancy probability of each possible value of the capacitances $C_j = \{C_A, C_B, C_C\}$. If the sequence of capacitance values is totally at random $\alpha = 0.5$ (white noise), the electrical transmission line is in the non-conducting state for every frequency ω. When we introduce long-range correlations in the distribution of capacitances, the electrical transmission lines can change their conducting properties and we can find a transition from the non-conducting to conducting state for a fixed system size. This implies the existence of critical values of the map parameters for each correlation exponent α. By performing finite-size scaling we obtain the asymptotic value of the map parameters in the thermodynamic limit for any α. With these data we obtain a phase diagram for the symmetric ternary model, which separates the non-conducting state from the conducting one. This is the fundamental result of this Letter. In addition, introducing one or more impurities in random places of the long-range correlated distribution of capacitances, we observe a dramatic change in the conducting properties of the electrical transmission lines, in such a way that the system jumps from conducting to non-conducting states. We think that this behavior can be considered as a possible mechanism to secure communication.

1. Introduction

According to the localization theory of Anderson [1], in 3D system with uncorrelated distribution of disorder, all one-electron states are spatially localized with an exponentially decaying envelope with a characteristic localization length ξ, when the disorder strength is larger than a critical value. Instead, Mott and Twose [2] claimed that all states are localized in 1D for non-vanishing disorder.

Recently, analytical as well as numerical studies revealed that delocalized electronic states can exist in a one-dimensional disordered lattice with short-range [3–7] and long-range [8–17] correlations. In addition, from the scaling theory [21] it is well known that an infinitesimal disorder can cause localization of all states in one- and two-dimensional systems in the thermodynamic limit. A clear picture of the delocalization mechanism of the long-range correlations in the disorder appears in a work by Díaz et al. [22].

Experimental evidence of delocalization produced by correlated disorder has been shown in the study of microwave propagation through disordered waveguides [18] and subterahertz response of superconducting multilayer [19] and in semiconductor superlattices with intentional disorder [20].

In this work we propose to study the conducting behavior of classical electrical transmission lines with long-range correlated disorder in the distribution of capacitances $\{C_j\}$. The scaling theory is used to study the phase transition in the thermodynamics limit. We introduce the disorder from a random sequence with a power spectrum $S(k) \propto k^{-(2\alpha-1)}$, where $\alpha \geqslant 0.5$ is the correlation exponent. From this sequence we generate an asymmetric ternary map using two map parameters b_1 and b_2, which adjust the occupancy probability of each possible value of the capacitances $C_j = \{C_A, C_B, C_C\}$. If the sequence of capacitance values is totally at random $\alpha = 0.5$ (white noise), the electrical transmission line is in the non-conducting state for every frequency ω. When we introduce a long-range correlation in the distribution of capacitances by mean of the correlation exponent α (we use $\alpha \geqslant 0.55$ in the present work) and depending on the values of the ternary map parameters b_1 and b_2, electrical transmission lines can change their conducting properties and we can find a transition from the

* Corresponding author.
E-mail address: edmundolazon@gmail.com (E. Lazo).

0375-9601/$ – see front matter
doi:10.1016/j.physleta.2010.06.031

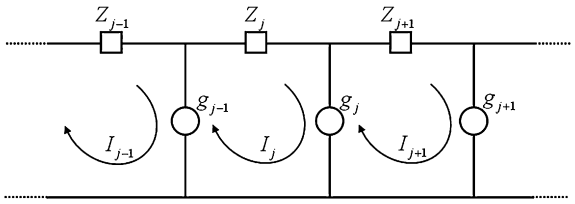

Fig. 1. Segment of an infinite electric circuit of classical impedances.

non-conducting to conducting state for a fixed system size. This implies the existence of critical values of the map parameters for each correlation exponent α. By performing finite-size scaling we obtain the asymptotic value of the map parameters b_1 and b_2 in the thermodynamics limit for any α. With these data we present below a phase diagram for the symmetric ternary model, which separates the non-conducting state from the conducting one. This is the fundamental result of this Letter.

In addition, introducing one or more impurities in random places of the long-range correlated distribution of capacitances, we observe a dramatic change in the conducting properties of the electrical transmission lines, in such a way that the system jumps from conducting to non-conducting states. We think that this behavior can be considered as a possible mechanism to secure communication.

Using classical circuits we can show the non-conducting to conducting transition, in analogy with the tight-binding formalism of quantum mechanics.

2. Model and method

We consider electrical circuits of classical impedances Z_j and g_j as shown in Fig. 1. Application of Kirchhoff's Loop Rule to three successive unit cells of the circuit leads to the following linear relation between the currents circulating in the $(j-1)$-th, j-th and $(j+1)$-th cells

$$(Z_j + g_{j-1} + g_j)I_j - g_{j-1}I_{j-1} - g_j I_{j+1} = 0 \tag{1}$$

2.1. Dual transmission line

Using the horizontal impedances being equal capacitances with $Z_j = (\frac{-i}{\omega C_j})$ and vertical impedances being equal to inductances with $g_j = (i\omega L_j)$, we obtain the equation for disordered dual transmission lines

$$d_j I_j - L_{j-1}I_{j-1} - L_j I_{j+1} = 0 \tag{2}$$

where $d_j = (L_{j-1} + L_j - \frac{1}{\omega^2 C_j})$. This equation describes the behavior of transmission lines with diagonal and non-diagonal disorder.

Eq. (2) takes the same form of the general equation of elementary excitations on a 1D chain with diagonal and off-diagonal disorder:

$$\alpha_j \phi_j - t_{j,j-1}\phi_{j-1} - t_{j,j+1}\phi_{j+1} = 0 \tag{3}$$

where ϕ_j represents the amplitude of the excitation at position j, α_j is a parameter which generally depends on the excitation energy E and other physical constants of the system, and $t_{j,j\pm1}$ describes the efficiency with which the excitation spreads from one point to another of the chain and, in general, also depends on the energy of the excitation. In particular, for the diagonal tight-binding Anderson model [1], relation (3) can be written as

$$(E - \varepsilon_j)\phi_j - \phi_{j-1} - \phi_{j+1} = 0 \tag{4}$$

where E is the eigenenergy and ε_j is the on-site energy. The Anderson model (4) gives an exact description of the diagonal disordered dual transmission lines when we consider in relation (2), that all inductances are the same: $L_j = L_0$, i.e.,

$$\left(2 - \frac{1}{\omega^2 L_0 C_j}\right) I_j - I_{j-1} - I_{j+1} = 0 \tag{5}$$

As a consequence, the correspondence between Anderson model (4) and disordered classical circuits (5), can be used to test the quantum effects of Anderson localization.

In this Letter, in order to study the transition from non-conducting to conducting states in disordered dual transmission lines, we use the Lyapunov exponent formalism. The Lyapunov exponent $\lambda(\omega)$ is a function of the frequency ω and can be defined as

$$\lambda(\omega) = \underset{N\to\infty}{Lim} \frac{1}{N}\sum_{j=1}^{N} \ln\left|\frac{I_{j+1}}{I_j}\right| \tag{6}$$

where I_j and I_{j+1} are the currents circulating in cells j and $(j+1)$, respectively. In the general case, dividing Eq. (2) by I_j, we obtain

$$d_j - L_{j-1}\frac{I_{j-1}}{I_j} - L_j\frac{I_{j+1}}{I_j} = 0 \tag{7}$$

Defining $\gamma_j = L_j\frac{I_{j+1}}{I_j}$, Eq. (7) can be put in the following recurrence form

$$\gamma_j = d_j - \frac{L_{j-1}^2}{\gamma_{j-1}} \tag{8}$$

Using relation (8) and the γ_j definition, we can write the Lyapunov exponent $\lambda(\omega)$ given by relation (6) in the following form

$$\lambda(\omega) = \underset{N\to\infty}{Lim} \frac{1}{N}\sum_{j=1}^{N} \ln\left|\frac{\gamma_j}{L_j}\right| \tag{9}$$

In this work we study the diagonal disordered dual transmission lines. In such case all inductances are the same: $L_j = L_0$ and the term $\frac{\gamma_j}{L_j}$ of Eq. (9) becomes $\overline{\gamma}_j = \frac{\gamma_j}{L_0}$. Dividing by L_0, the recurrence equation (8) can be written as

$$\overline{\gamma}_j = \bar{d}_j - \frac{1}{\overline{\gamma}_{j-1}} \tag{10}$$

where $\overline{\gamma}_{j-1} = \frac{\gamma_{j-1}}{L_0}$ and $\bar{d}_j = \frac{d_j}{L_0} = 2 - \frac{1}{\omega^2 L_0 C_j}$. Using $C_j = \alpha_j C_0$, we have

$$\overline{\gamma}_j = \left(2 - \frac{1}{\omega^2 L_0 C_0 \alpha_j}\right) - \frac{1}{\overline{\gamma}_{j-1}} \tag{11}$$

Defining $\overline{\omega} = (\omega\sqrt{L_0 C_0})$ as the frequency measured in units of $(\frac{1}{\sqrt{L_0 C_0}})$, we finally write the recurrence equation in the following way

$$\overline{\gamma}_j = \left(2 - \frac{1}{\overline{\omega}^2 \alpha_j}\right) - \frac{1}{\overline{\gamma}_{j-1}} \tag{12}$$

In this way, the correlated disorder introduced in the sequence of capacitances $C_j = \{C_A, C_B, C_C\}$ given by the ternary map, is now introduced in the coefficient α_j, because $C_j = \{\alpha_A, \alpha_B, \alpha_C\}C_0$. In all numerical calculations and in all figures we use the symbol ω as the frequency measured in units of $(\frac{1}{\sqrt{L_0 C_0}})$. The Lyapunov exponent $\lambda(\omega)$ is a suitable tool to describe conduction properties through the transmission line, because it is related to the exponential decrease of the electric current function. The localization length $\xi(\omega)$ is defined as the inverse of the Lyapunov exponent:

$$\xi(\omega) = \frac{1}{\lambda(\omega)} \tag{13}$$

This relation gives the single value of $\xi(\omega)$ only for the infinite system size $N \to \infty$. However, when N is finite, the calculated result of Eq. (13) – denoted as ξ_N – depends on the choice of the sequence of capacitances $\{C_j\}$. To obtain a typical value of ξ_N for a given N, we take the mean of ξ_N over 5000 samples from which we define the normalized localization length $\Lambda = \frac{\xi_N}{N}$ on the system size N. In this work we use the localization length Λ to characterize conducting or non-conducting states using the following criteria for a fixed number of cells N in the transmission lines: if $\Lambda(\omega) \geqslant 1$ we have a conducting transmission line for the frequency ω because $\xi_N \geqslant N$, and if $\Lambda(\omega) < 1$, we have a non-conducting transmission line for the frequency ω because $\xi_N < N$. The non-conducting (conducting) states in disordered transmission lines are analogous to the localized (delocalized) states in 1D disordered quantum system. In all numerical calculations, the possibility of a phase transition from non-conducting to conducting transmission lines is investigated for a fixed frequency $\omega = 3.6$. However, in the thermodynamic limit, $N \to \infty$, we have verified that the results do not change when we use a different frequency $\omega' \neq \omega$. In this work we study the diagonal disordered model, which means that we do $L_j = L_0$, $\forall j$.

2.2. Long-range correlated disorder

We want to study the localization properties of a ternary model with long-range correlated disorder. Thus, we need first to generate numerical long-range correlated sequences $\{v_j\}$ to build the ternary map. A sequence of long-range correlated terms $\{v_j\}$ is produced by the Fourier filtering method [23]. This method initially uses a set of numbers $\{u_j\}$ which are uncorrelated random numbers with a Gaussian distribution. After that, we take the fast Fourier transform (FFT) of the random sequence $\{u_j\}$, obtaining the sequence $\{u_k\}$. Now we introduce the long-range correlation by means of the following process

$$v_k = u_k k^{-(2\alpha-1)/2} \tag{14}$$

defining in this way a new sequence $\{v_k\}$. Finally we calculate the inverse FFT of $\{v_k\}$, obtaining $\{v_j\}$. This sequence is spatially correlated with the spectral density

$$S(k) \propto k^{-(2\alpha-1)} \tag{15}$$

The exponent α is called correlation exponent and quantifies the degree of long-range correlation imposed in the system. With this definition, α corresponds to the exponent provided by Detrended Fluctuation Analysis (DFA), which is one of the most widely used methods to quantify long-range correlations [24–26]. The case $\alpha = 0.5$ corresponds to the uncorrelated disorder (white noise), while the case $\alpha > 0.5$ indicated positive correlations. As a last step we normalize the sequence $\{v_j\}$ to obtain zero average, $\langle v_j \rangle = 0$ and the variance is set to unity. We have confirmed that the sequences $\{v_j\}$ produce the power-law spectral density $S(k) \propto k^{-(2\alpha-1)}$ for all $\alpha \geqslant 0.5$. With this normalized sequence $\{v_j\}$ we build the asymmetric ternary models. The asymmetric model is generated by means of a transformation which maps the elements of the normalized long-range correlated sequence $\{v_j\}$ into three different values of capacitances $C_j = \{C_A, C_B, C_C\}$.

2.3. The asymmetric ternary model

The sequence of capacitances $\{C_j\}$ of the asymmetric ternary model is given by

$$C_j = \begin{cases} C_A & \text{if } v_j < b_1 \\ C_C & \text{if } b_1 \leqslant v_j \leqslant b_2 \\ C_B & \text{if } v_j > b_2 \end{cases} \tag{16}$$

with $b_2 \geqslant b_1$. The symmetric ternary case [14] corresponds to $b_2 = -b_1 = b$ and $b > 0$.

The asymmetric binary map can be obtained for $b_2 = b_1 = b$

$$C_j = \begin{cases} C_A & \text{if } v_j < b \\ C_B & \text{if } v_j \geqslant b \end{cases} \tag{17}$$

In the limit $b \to 0$, we obtain the symmetric binary map.

Binary (17) and ternary (16) maps can change the correlation properties of the sequence $\{v_j\}$, and therefore, the correlation of the sequence $\{C_j\}$ is not properly quantified by the correlation exponent α in the original correlated sequence $\{v_j\}$.

The metal–insulator transition in binary and ternary symmetrical model for 1D tight-binding systems has been studied in Refs. [9,11] and [14], respectively.

2.4. The finite-size scaling

An effective identification of critical points of finite systems is the finite-size scaling [27–29]. Finite-size scaling characterizes the scaling behavior of thermodynamic quantities of finite system near a critical point. The main points of the finite-size scaling can be described as the following. An observable Q of a finite system is a function of a critical parameter P and system size N. When N is much larger that the microscopic length scale and P is in the vicinity of critical point P_c, the observable $Q(P, N)$ can be written in the finite-size scaling form [30]

$$Q(P, N) = N^{\frac{\lambda}{\nu}} F_Q\left(tN^{\frac{1}{\nu}}\right) \tag{18}$$

where $t = (P - P_c)/P_c$ is the reduced critical parameter and λ is the critical exponent of the observable Q and ν is the critical exponent of the correlation length $\xi = \xi_0 t^{-\nu}$.

Using finite-size scaling we can find the critical point. At critical point $P = P_c$, the reduced critical parameter t goes to zero, $t = 0$, and relation (18) becomes

$$Q(P_c, N)N^{-\frac{\lambda}{\nu}} = F_Q(0) \tag{19}$$

where the finite-size scaling function $F_Q(0)$ is constant and independent of the system size N. In the plot of $Q(P, N)N^{-\frac{\lambda}{\nu}}$ *versus* P, the critical point $[P_c, F_Q(0)]$ is a fixed point, where all curves of different system sizes converge to. Reversely, the appearance of a fixed point indicates the existence of a critical point. Using this behavior, the critical point can be found from the system size dependence of the observable.

In another way, taking the logarithm of relation (18), we have

$$\ln Q(P, N) = \frac{\lambda}{\nu} \ln N + \ln F_Q\left(tN^{\frac{1}{\nu}}\right) \tag{20}$$

At critical point, $P = P_c$ and $t = 0$, the finite-size scaling function $F_Q(0)$ is constant and, consequently, the term $\ln F_Q(tN^{\frac{1}{\nu}})$ becomes a constant. This mean that $\ln Q(P_c, N)$ becomes a straight line with respect to $\ln N$. When the system is away from the critical point, i.e., $P \neq P_c$ and $t \neq 0$, the function $F_Q(tN^{\frac{1}{\nu}})$ depends on the critical parameter P and on the system size N. In this case the relation (20) does not represent a straight line.

In this work we can use the finite-size scaling considering, as the observable Q, the normalized localization length Λ, i.e., $Q = \Lambda$. In general, $\Lambda = \Lambda(\omega, b, \alpha, N)$, depends on the frequency ω, the map parameter b (for the symmetric ternary model), the correlation exponent α and the system size N. In our case, the parameters b and α can be considered as critical parameters. When we use the map parameter b as the critical parameter for a fixed

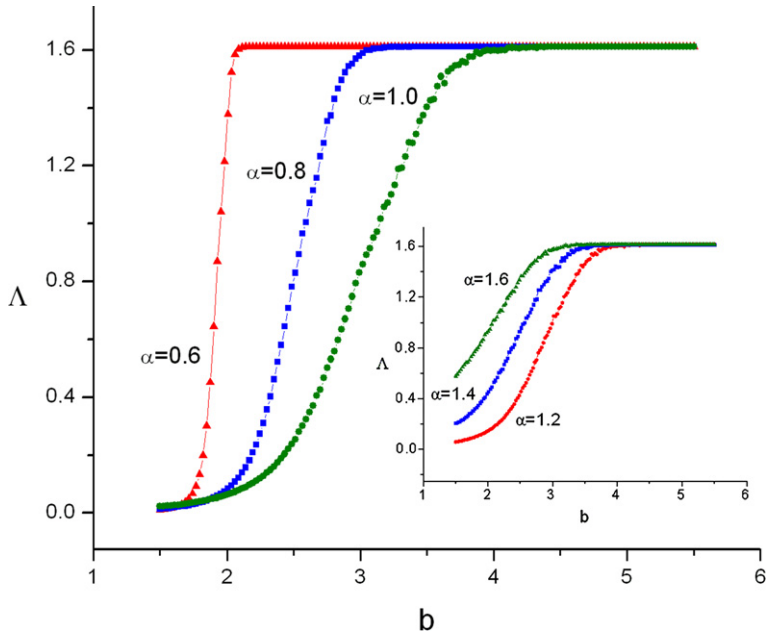

Fig. 2. Normalized localization length $\Lambda(b, N)$ as a function of the parameter b, for fixed frequency $\omega = 3.6$ and different correlation exponents $\alpha = \{0.6, 0.8, 1.0\}$ for a fixed system size $N = 2^{15}$. The inset shows the same situation, but for $\alpha = \{1.2, 1.4, 1.6\}$.

correlation exponent α, there exist only one critical points b_c. However, when we use the correlation exponent α as the critical parameter for a fixed map parameter b, there are two critical points α_{c_1} and α_{c_2} with $\alpha_{c_1} < \alpha_{c_2}$ (see the phase diagram below).

If we consider the map parameter b as the critical parameter, i.e., $P = b$, for a fixed correlation exponent α and a fixed frequency ω, the fixed point can be found by investigating the dependence of the function $\Lambda(b, N)N^{-\beta}$ of parameter b for different system sizes. When a fixed point is observed, at a certain parameter β, it indicates the existence of a critical point and the parameter β is related to the ratio of critical exponents, i.e., $\beta = \frac{\lambda}{\nu}$ of the relation (19).

3. Numerical results

3.1. The symmetrical map

In this work we study numerically the localization properties of dual transmission lines when the long-correlated disorder is obtained from the symmetric ternary maps: $b_2 = -b_1 = b$ and $b > 0$. In all numerical calculations, the possibility of a phase transition in the thermodynamic limit from non-conducting to conducting transmission lines is investigated for a fixed frequency $\omega = 3.6$.

In this work we use the ternary symmetrical map parameter b as the critical parameter, i.e., $b = b(\alpha)$ as a function of the correlation exponent α. In this way, we numerically study the behavior of the observable $\Lambda(b, N)$ on the system size N. The critical point $b = b_c$ permits us to discriminate between non-conducting states from conducting states. Fig. 2 plots $\Lambda(b, N)$ as a function of the parameter b, for a fixed frequency $\omega = 3.6$ and different correlation exponents $\alpha = \{0.6, 0.8, 1.0\}$ for a fixed system size $N = 2^{15}$. The inset shows the same situation for $\alpha = \{1.2, 1.4, 1.6\}$. For each correlation exponent α, the normalized localization length $\Lambda(b, N)$ is a growing function of the parameter b, until a critical point $b = b_c$ appears. For $b > b_c$, $\Lambda(b, N)$ is practically independent of b.

Fig. 3 shows the normalized localization length $\Lambda(b, N)$ as a function of the map b parameter for a fixed $\alpha = 0.7$, for different system sizes $N = \{2^{17}, 2^{18}, 2^{19}\}$. In this case, all curves change their behavior near a critical point. This critical point corresponds to a finite system size N. In the thermodynamic limit, the critical value $b_c(\alpha)$ will be found using the finite-size scaling method.

Fig. 4 shows the normalized localization length $\Lambda(\omega)$ as a function of the frequency ω for $\alpha = 0.7$ and three different values of the parameter $b = \{2.1, 2.2, 2.3\}$, for a fixed system size $N = 2^{15}$. In all graphs $\Lambda(\omega)$ versus ω of this work, we have averaged over ten frequency values to avoid large fluctuations in the value of $\Lambda(\omega)$. In Fig. 4 we clearly can see that the curve $\Lambda(\omega)$ is a growing function of the parameter b. For $b = 2.1$ and $b = 2.2$ we have $\Lambda(\omega) < 1$, i.e., $\xi_N < N$ and the dual transmission line is in the non-conducting state for every frequency ω. For $b = 2.3$, a portion of the curve $\Lambda(\omega)$ satisfies the condition $\Lambda(\omega) \geqslant 1$, i.e., $\xi_N \geqslant N$. In this case we can say that the transmission line is in the conducting state, because the average localization length ξ_N is greater than the system size N for a certain band of frequency values. As a consequence, there is a critical parameter b_c, such that for $b > b_c$, it can be observed a mobility edges separating non-conducting states from conducting ones. It means that there exists a continuum spectrum of conducting states, at least for a finite system size N of the dual transmission lines.

To characterize the scaling behavior of $\Lambda(b, N)$ for a finite system size near critical point, we will use the finite-size scaling. To do that, for a fixed correlation exponent α, we can write the relation (19) in the following form

$$\Lambda(b, N)N^{-\beta} = F_{\Lambda}(0) \tag{21}$$

where β is the critical exponent. In this way, we can find the fixed points b_c for each α value, varying the critical exponent β. Fig. 5 shows the presence of a fixed point $b_c \approx 2.54$ for $\alpha = 0.7$ and $\omega = 3.6$ for various system sizes ranging from $N = 2^{17}$ to 2^{20}, for a specific critical exponent β_0. In this fixed point $b_c \approx 2.54$, a convergence of all curves for different sizes N can be observed.

In addition, using relation (20), the scaling relation for the normalized localization length $\Lambda(b, N)$, can be written as

$$\ln \Lambda(b, N) = \beta \ln N + \ln F_{\Lambda}\left(tN^{\frac{1}{\nu}}\right) \tag{22}$$

where now $t = \frac{b - b_c}{b_c}$ is the b reduced critical parameter. The critical point $b = b_c$ can be found studying the system size dependence of $\ln \Lambda(b, N)$ for different values of the map parameter b. At criti-

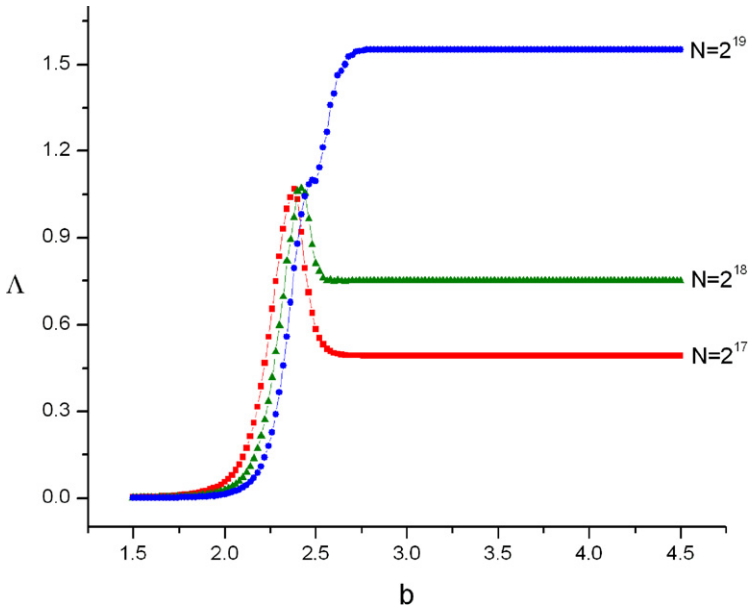

Fig. 3. Normalized localization length $\Lambda(b, N)$ as a function of the map parameter b for fixed correlation exponent $\alpha = 0.7$, for different system sizes $N = \{2^{17}, 2^{18}, 2^{19}\}$. In this case, all curves qualitatively change their behavior near a critical point ($b_c \approx 2.5$).

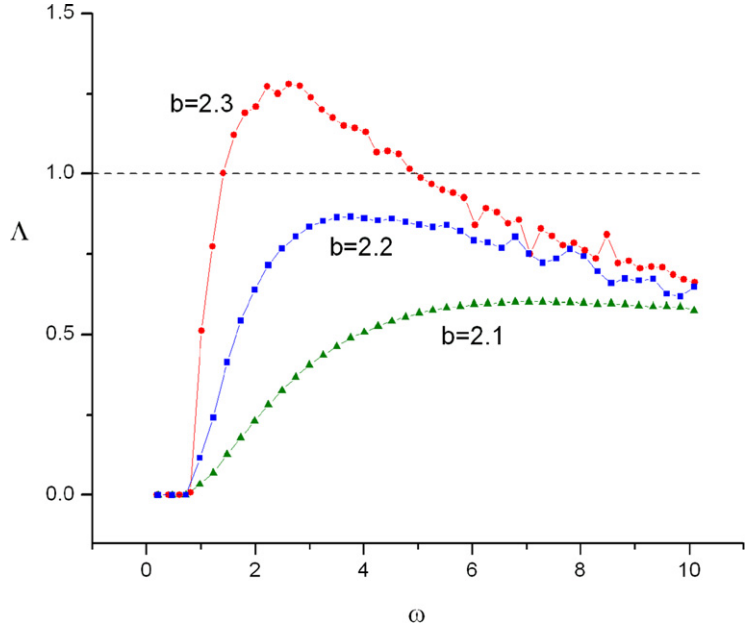

Fig. 4. Normalized localization length $\Lambda(\omega, N)$ as a function of the frequency ω for $\alpha = 0.7$ and three different values of the parameter $b = \{2.1, 2.2, 2.3\}$, for fixed system size $N = 2^{15}$.

cal point, $b = b_c$ ($t = 0$), in this case $\ln \Lambda(b_c, N)$ becomes a straight line with respect to $\ln N$, because $\ln F_\Lambda(0)$ becomes a constant.

Using relation (22), we have found every critical point $b_c(\alpha)$ at thermodynamical limit. Fig. 6 shows the typical behavior for the case $\alpha = 0.7$, $\omega = 3.6$, when the system size varies from $N = 2^{17}$ to $N = 2^{20}$. There we can see that the best straight line (with a correlation coefficient $R = 0.99985$) occurs when $b = b_c = 2.54$. In our work, all critical points $b_c(\alpha)$ were found with a correlation coefficient greater than 0.999.

In this way, using the finite-size scaling method, we have found all the critical points $b_c(\alpha)$ which separate non-conducting states from conducting states of the dual disordered transmission lines. With these data we have found the phase diagram shown in Fig. 7. This phase diagram is the main result of this Letter, and contains all the information of the conducting properties of the disordered dual transmission lines when the disorder is given by a long-range correlated symmetric ternary model, which is characterized by the symmetric map b parameter and the correlation α exponent. The plotted points in Fig. 7 correspond to values of the correlation exponent $\alpha \geqslant 0.55$, i.e., the disordered systems which we have studied always presents long-range correlation. The case $\alpha = 0.5$ corresponds to an uncorrelated disorder (white noise) and, therefore, the disordered system is in the non-conducting regime.

3.2. The asymmetrical map

For the asymmetric ternary map (16) where $b_1 \neq b_2$, the long-range correlated ternary model behaves in a way very similar to the symmetric ternary map just studied. However, a calculation of the complete phase diagram for parameters b_1, b_2 and α, is of

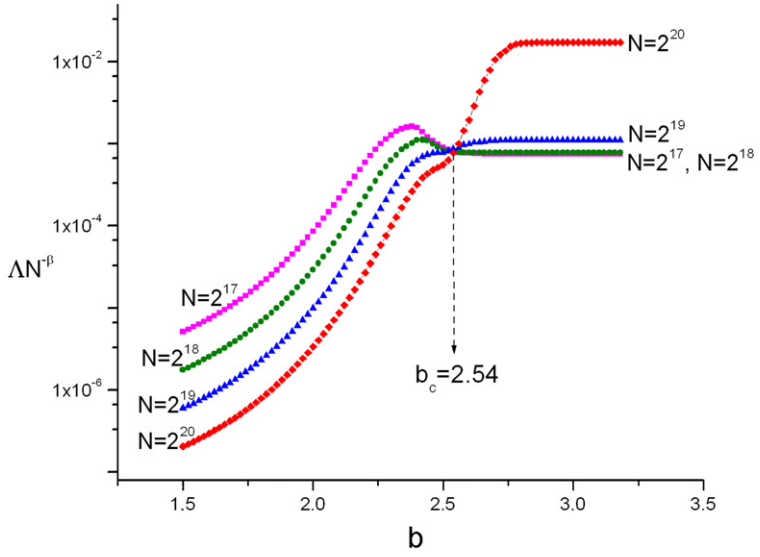

Fig. 5. Scaling plot of $(\Lambda(b,N)N^{-\beta})$ versus the map b parameter for $\alpha = 0.7$ and $\omega = 3.6$ for various system sizes N. For a specific critical exponent β_0, a fixed point appears ($b_c \approx 2.54$), where all curves of different system sizes converge.

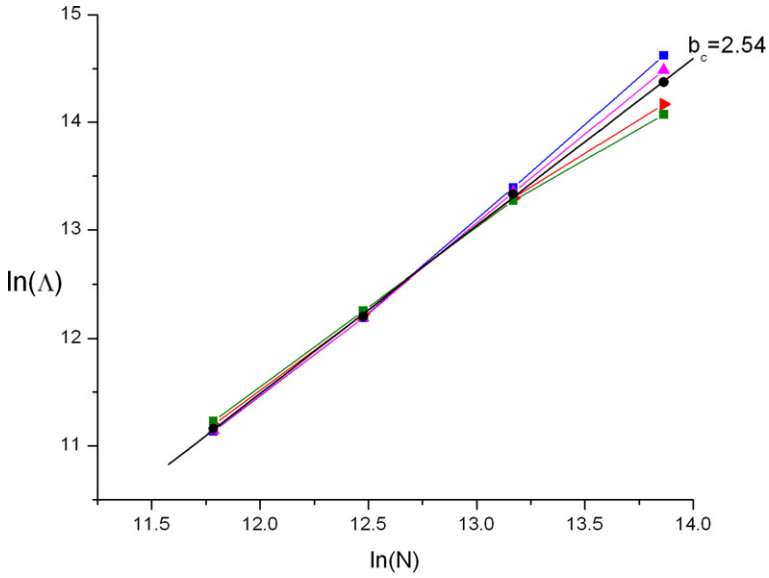

Fig. 6. Scaling plot of $\ln(\Lambda(b,N))$ versus $\ln(N)$ for $\alpha = 0.7$, $\omega = 3.6$, for different b values when the system size varies from $N = 2^{17}$ to $N = 2^{20}$. The best straight line (with a correlation coefficient $R = 0.99985$) occurs when the critical point is $b_c = 2.54$.

great difficulty and out of the scope of the present manuscript. Fig. 8 shows the behavior of the normalized localization length $\Lambda(\omega)$ as a function of the frequency ω for the case $b_1 = -0.9$, $b_2 = 1.7$ for different correlation exponents $\alpha = \{1.7, 1.8, 2.0, 2.6\}$. There we can see bands of continuum spectrum of conducting states for $\alpha = 2.0$ and $\alpha = 2.6$, for finite system size $N = 2^{15}$, in a similar way to the behavior observed in Fig. 4 for the ternary symmetric map.

3.3. The symmetric binary map

In addition, we have studied the special case $b_1 = b_2 = 0$, corresponding to the symmetric binary map (17). In this case, using the finite-size scaling, we have found conducting bands in the dual transmission lines for correlation exponent $\alpha \geqslant 2.0$. For binary map in 1D tight-binding systems, the conducting bands appear for $\alpha \geqslant 1.5$ (see Refs. [9,11]).

In summary, when we use binary or ternary maps (symmetric or asymmetric) to generate the distribution of capacitances $\{C_j\}$ in the dual classical transmission lines, we obtain bands of continuum spectrum of conducting states for certain values of the correlation exponent α and the map parameters b_1 and b_2.

3.4. Secure communication

Let us consider a transmission line which is in the conducting state for a specific value of the correlation exponent α and the map parameters b_1 and b_2. If we introduce one or more capacitance values C_r generated at random (impurities) in random places of the transmission line, breaking in this way the long-range correlated sequence of capacitors, which are the changes in the normalized localization $\Lambda(\omega)$? Fig. 9 shows the numerical answer to this question. There we show the normalized localization length $\Lambda(\omega)$ as a function of the frequency ω for the ternary asymmetric case $b_1 = -0.9$, $b_2 = 1.7$, with correlation exponent $\alpha = 1.9$, for finite system size $N = 2^{15}$. We compare the case without random capacitances C_r (0 random) with the cases with one, two and three random capacitances C_r (n random). The effect of break-

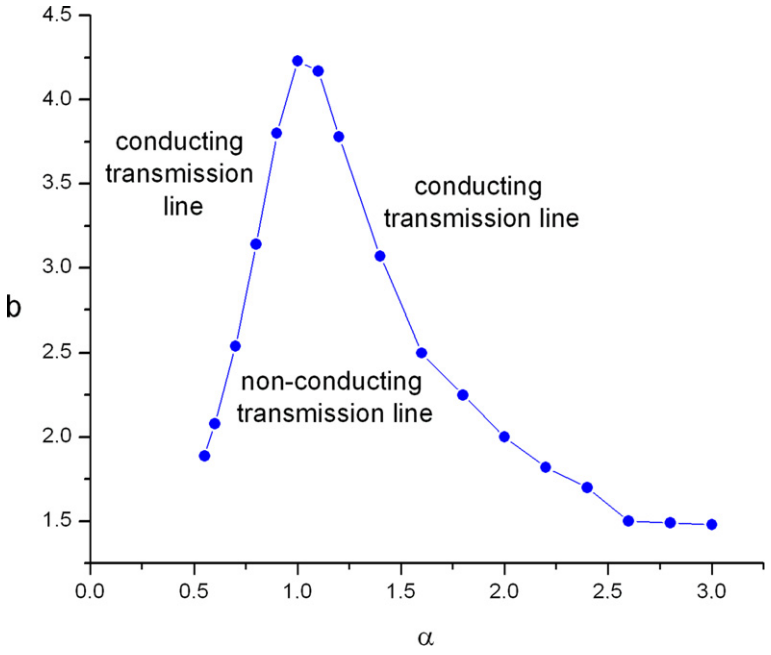

Fig. 7. Phase diagram separating non-conducting from conducting states in the thermodynamics limit in terms of the symmetric map parameter $b_c(\infty)$ as a function of the correlation exponent α. The plotted points correspond to values of the correlation exponent $\alpha \geqslant 0.55$, i.e., the disordered system always presents long-range correlation.

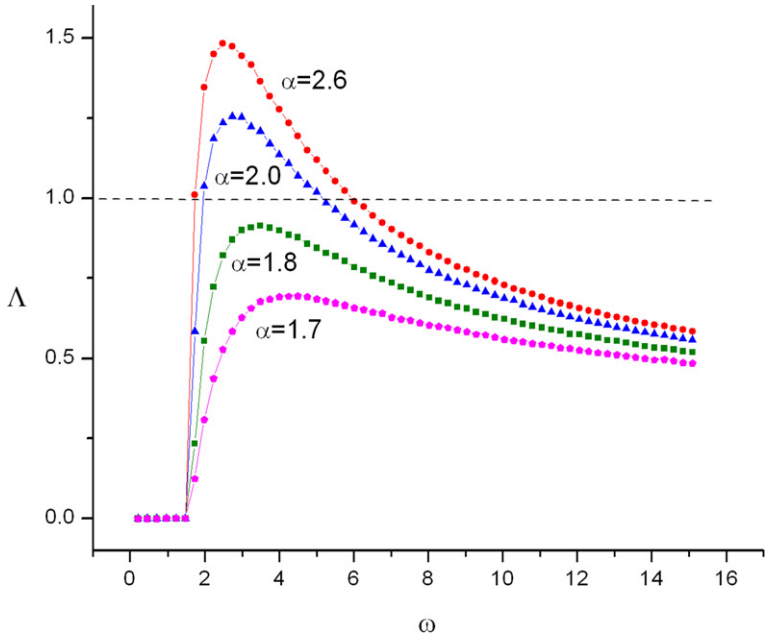

Fig. 8. Normalized localization length $\Lambda(\omega)$ as a function of the frequency ω for the asymmetric ternary map when $b_1 = -0.9$, $b_2 = 1.7$ for different correlation exponents $\alpha = \{1.7, 1.8, 2.0, 2.6\}$.

ing the long-range correlated sequence of capacitors with n random capacitances is remarkable, since the introduction of at least one impurity (1 random), the normalized localization length $\Lambda(\omega)$ jumps from the conducting state ($\Lambda \geqslant 1$) to a non-conducting state ($\Lambda < 1$). When putting two or more impurities, the long-range correlation tends to be destroyed almost completely. As a consequence, the dual transmission line becomes a non-conducting system. This is an interesting effect that can be used in secure communication, because any alteration of the long-range correlated sequence by means of a change in the capacitance of any capacitor, in any place of the transmission line, reduces drastically the conducting band or even the transmission line jumps from a conducting state to a non-conducting state. See Ref. [31] for a new method to secure communications, which does not require coding and decoding of the transmitting signal.

4. Conclusion

In summary, we have studied the classical dual transmission lines introducing long-range correlated disorder by means of the symmetric and asymmetric ternary model used to generate the sequence of capacitances $\{C_A, C_B, C_C\}$. For a given correlation exponent α of the original sequence, the normalized localization length $\Lambda(b_1, b_2, N)$ depends on the asymmetric parameters b_1 and b_2 in a complicated way, and they are responsible for the phase transition from non-conducting to conducting states of the dual trans-

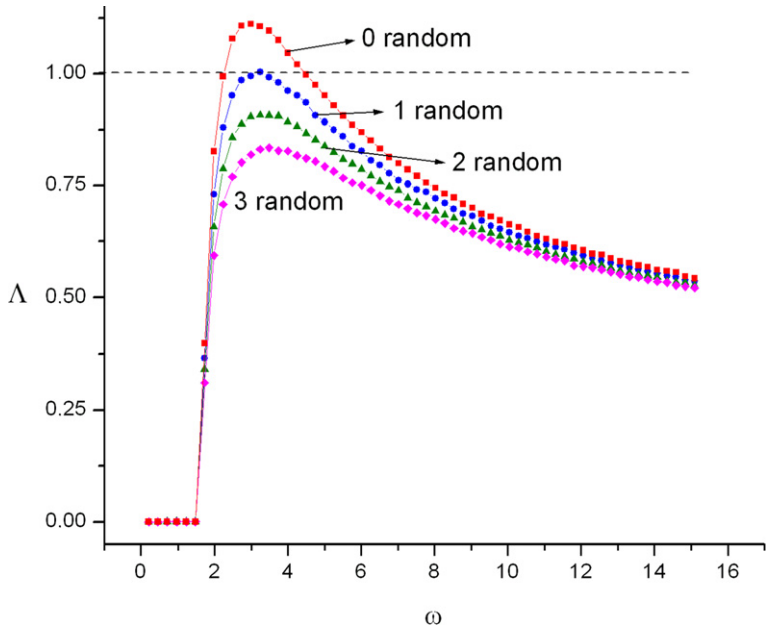

Fig. 9. Normalized localization length $\Lambda(\omega)$ as a function of the frequency ω for the ternary asymmetric map for $b_1 = -0.9$, $b_2 = 1.7$, with correlation exponent $\alpha = 1.9$, for a finite system size $N = 2^{15}$. We compare the conducting case without impurities (0 random), with the case with one or more impurities (n random). The introduction of one or more impurities (n random), produces a relevant jump from conducting state ($\Lambda \geqslant 1$) to a non-conducting state ($\Lambda < 1$).

mission lines. By performing finite-size scaling, we find that the transition is not a finite-size effect, because we were able to calculate each critical map b parameter at the thermodynamics limit b_c for every correlation exponent α. With these data we obtained the phase diagram for the symmetric ternary map, which is the fundamental result of this work. In addition, the asymmetric ternary map presents a great sensibility to any change in the long-range correlated sequence of capacitances, because any minimal alteration of the original sequence produces a drastic decrease in the normalized localization $\Lambda(b, N)$, which means that the classical dual transmission line jumps from conducting to non-conducting state in certain cases. This is an interesting effect that can be used in secure communication.

Acknowledgements

E. Lazo acknowledges the support of this research by the Dirección de Investigación y Extensión Académica de la Universidad de Tarapacá, under project No. 4720-07. E. Diez acknowledges the financial support of this research by the Cariplo Foundation (project QUANTDEV) and by the Spanish Ministry of Science and Innovation (FIS2009-07880, PPT310000-2009-6, PCT310000-2009-3) and Junta de Castilla y León (SA049A10).

References

[1] P.W. Anderson, Phys. Rev. 109 (1958) 1492.
[2] N.F. Mott, W.D. Twose, Adv. Phys. 10 (1961) 107.
[3] J.C. Flores, J. Phys.: Condens. Matter 1 (1989) 8471.
[4] D.H. Dunlap, H.L. Wu, P.W. Philips, Phys. Rev. Lett 65 (1990) 88;
P.W. Philips, H.-L. Wu, Science 252 (1991) 1805.
[5] E. Lazo, M.E. Onell, Physica B 299 (2001) 173.
[6] W. Zhang, S.E. Ulloa, Phys. Rev. B 69 (2004) 153203.
[7] M. Titov, H. Schomerus, Phys. Rev. Lett. 95 (2005) 126602.
[8] J.M. Luck, Phys. Rev. B 39 (1989) 5834.
[9] F.A.B.F. de Moura, M.L. Lyra, Phys. Rev. Lett. 81 (1998) 3735;
F.A.B.F. de Moura, M. Lyra, Physica A (Amsterdam) 266 (1999) 465.
[10] J.W. Kantelhardt, S. Russ, A. Bunde, S. Havlin, I. Webman, Phys. Rev. Lett. 84 (2000) 198.
[11] F.M. Izrailev, A.A. Krokhin, Phys. Rev. Lett. 82 (1999) 4062;
F.M. Izrailev, A.A. Krokhin, S.E. Ulloa, Phys. Rev. B 63 (2001) 041102(R);
F.M. Izrailev, N.M. Makarov, J. Phys. A 38 (2005) 10613.
[12] P. Carpena, P.B. Galvan, P.Ch. Ivanov, H.E. Stanley, Nature 418 (2002) 955;
P. Carpena, P.B. Galvan, P.Ch. Ivanov, H.E. Stanley, Nature 421 (2003) 764.
[13] H. Shima, T. Nomura, T. Nakayama, Phys. Rev. B 70 (2004) 075116;
H. Shima, T. Nakayama, Microelectronic J. 36 (2005) 422.
[14] A. Esmailpour, M. Esmaeilzadeh, E. Faizabadi, P. Carpena, M. Reza Rahimi Tabar, Phys. Rev. B 74 (2006) 024206;
A. Esmailpour, H. Cheraghchi, P. Carpena, M. Reza Rahimi Tabar, J. Stat. Mech. (2007) P09014.
[15] T. Kaya, Eur. Phys. J. B 55 (2007) 49.
[16] R. Benhenni, K. Senouci, N. Zekri, R. Bouamrane, arXiv:0906.2402v2 [cond-mat].
[17] Y. Zhao, S. Duan, W. Zhang, arXiv:0908.3871v1 [cond-mat].
[18] U. Kulh, F.M. Izrailev, A.A. Krokhin, H.-J. Stöckmann, Appl. Phys. Lett. 77 (2000) 633.
[19] V.A. Yampol'skii, S. Savel'ev, O.V. Usatenko, S.S. Mel'nik, F. Kusmartsev, A.A. Krokhin, F. Nori, Phys. Rev. B 75 (2007) 014527.
[20] V. Bellani, E. Diez, R. Hey, L. Toni, L. Tarricone, G.B. Parravicini, F. Dominguez-Ademe, R. Gómez-Alcalá, Phys. Rev. Lett. 82 (1999) 2159.
[21] E. Abrahams, P.W. Anderson, D.G. Licciardello, T.V. Ramakrishnan, Phys. Rev. Lett. 42 (1979) 673.
[22] E. Díaz, A. Rodríguez, F. Domínguez-Adame, V.A. Malyshev, Europhys. Lett. 72 (2005) 1018.
[23] C.-K. Peng, S. Havlin, M. Schwartz, H.E. Stanley, Phys. Rev. A 44 (1991) 2239;
H.A. Makse, S. Havlin, M. Schwartz, H.E. Stanley, Phys. Rev. E 53 (1996) 5445.
[24] K. Hu, Z. Chen, P.-Ch. Ivanov, P. Carpena, H.E. Stanley, Phys. Rev. E 64 (2001) 011114.
[25] Z. Chen, et al., Phys. Rev. E 71 (2005) 01110.
[26] A.V. Coronado, P. Carpena, J. Biol. Phys. 31 (2005) 121.
[27] M.E. Fisher, in: M.S. Green (Ed.), Critical Phenomena, in: Proceeding of the International School of Physics Enrico Fermi, Course 51, Academic, New York, 1971.
[28] E. Brézin, J. Phys. (Paris) 43 (1982) 15.
[29] X.S. Chen, V. Dohm, A.L. Talapov, Physica A 232 (1996) 375;
X.S. Chen, V. Dohm, A.N. Schultka, Phys. Rev. Lett. 77 (1996) 3641.
[30] Ch. Lizhu, X.S. Chen, W. Yuanfang, arXiv:0904.1040v1 [nucl-th].
[31] E. Diez, F. Izrailev, A. Krokhin, A. Rodriguez, Phys. Rev. B 78 (2008) 035118.